MiR-146a-5p Targeting SMAD4 and TRAF6 Inhibits Adipogenesis Through TGF-β and NF-κB Signal Pathways in Porcine Intramuscular Preadipocytes

Que Zhang
Northwest Agriculture and Forestry University
Rui Cai
Northwest Agriculture and Forestry University
Guorong Tang
Northwest Agriculture and Forestry University
Wanrong Zhang
Northwest Agriculture and Forestry University
Weijun Pang (pwj1226@nwsuaf.edu.cn)
Northwest Agriculture and Forestry University

Research

Keywords: MiR-146a-5p, porcine intramuscular fat, adipogenesis, SMAD4, TRAF6, TGF-β signal pathway, NF-κB signal pathway

Posted Date: June 30th, 2020

DOI: https://doi.org/10.21203/rs.3.rs-38947/v1

Version of Record: A version of this preprint was published on February 3rd, 2021. See the published version at https://doi.org/10.1186/s40104-020-00525-3.

Abstract

Background: Intramuscular fat (IMF) content is a vital parameter to assess pork quality. Increasing evidences have shown that microRNAs (miRNAs) play an important role in regulating porcine IMF deposition. Here, a novel miRNA implicated in porcine IMF adipogenesis was found, and its effect and regulatory mechanism was further explored on the proliferation and differentiation of intramuscular preadipocytes.

Results: By miRNAs sequencing analysis in porcine adipose tissues, we found that miR-146a-5p was a potential regulator of porcine IMF adipogenesis. Further study showed that miR-146a-5p mimics inhibited the proliferation of porcine intramuscular preadipocytes, but its inhibitor promoted cell proliferation. Interestingly, miR-146a-5p mimics also repressed preadipocyte differentiation, whereas its inhibitor promoted adipogenic differentiation. Mechanistically, miR-146a-5p suppressed cell proliferation by directly targeting SMAD family member 4 (*SMAD4*) to attenuate the TGF-β signal. Moreover, miR-146a-5p inhibited the differentiation of intramuscular preadipocytes by targeting TNF receptor associated factor 6 (*TRAF6*) to weaken the NF-κB signaling of the *TRAF6* downstream pathway.

Conclusions: MiR-146a-5p targeting *SMAD4* and *TRAF6* inhibited porcine intramuscular adipogenesis through attenuating TGF-β and NF-κB signals, respectively. These findings provided a novel miRNA biomarker for regulating intramuscular adipogenesis to promote pork quality.

Background

Intramuscular fat (IMF) content implicated in pork tenderness, flavor and juiciness is an important indicator to assess the quality characteristics of pork [1, 2]. How to properly increase IMF content and improve pork quality has become a hot topic in recent years [3]. IMF deposition is achieved by the proliferation and differentiation of intramuscular preadipocytes [4]. The proliferation of preadipocytes is regulated by the differential expression of cell cycle regulators, including cyclin-dependent kinases (*CDKs*), CDK inhibitors (*CKIs*) and other transcription factors [5]. Similarly, the preadipocyte differentiation process also involves many regulatory factors, including peroxisome proliferator-activated receptor γ (*PPARγ*), CCAAT / enhancer binding protein (*C/EBP*) family, fatty acid binding protein 4 (*FABP4*), and lipoprotein lipase (*LPL*) [6]. However, besides above key genes, many identified miRNAs by RNA-seq are also involved in the regulation of porcine IMF content, their function and mechanism need further study.

MiRNAs are small, evolutionarily conserved, non-coding RNAs that have an important function in the regulation of gene expression. MiRNAs function generally by binding target genes that match their “seed sequences” to suppress or degrade target gene mRNA after transcription and coordinate normal processes, including cellular proliferation, differentiation and apoptosis [7, 8]. Increasing evidence showed that miRNAs, including miR-206 [9], miR-149-5p [10] and miR-204-5p [11] played key roles in the process of preadipocyte proliferation and differentiation. Moreover, many miRNAs that are differentially expressed in porcine adipose tissue during different developmental stages have been excavated by

transcriptome sequencing technology [12]. We therefore speculated that these above miRNAs may be key regulators of porcine IMF deposition by their target genes.

The classical TGF-β/SMAD signal regulates cell proliferation, differentiation, migration and growth. SMAD4, as an important transmission medium, transduced extracellular signals including TGF-β and BMP to the nucleus [13–15]. Literatures indicated that *SMAD4* regulated proliferation and migration of A549 cells [16], and Dihydromyricetin inhibited the proliferation of human choriocarcinoma JAR cells via downregulation *SMAD4* expression level [17], and miR-224 mediated the proliferation of HCT116 cells by targeting *SMAD4* [18]. Although *SMAD4* has been discovered and studied in proliferation of different types of cells, it needs further explore whether *SMAD4* is implicated in proliferation of porcine intramuscular preadipocytes.

TRAF6 is an important intracellular multifunctional signaling molecule, which has unique receptor binding specificity [19]. Through a series of signal transmission, TRAF6 finally activates nuclear factor NF-κB participating in cell proliferation, differentiation, embryonic development and bone metabolism [20]. At present, *TRAF6* has been studied on obesity or adipogenesis. The mRNA and protein levels of TRAF6 significantly increased in obese mice after high-fat feeding for 6 weeks [21]. Oleanolic acid inhibited visfatin and its inflammatory response during preadipocyte differentiation by blocking IL-6/TRAF6/NF-κB signaling [22]. Furthermore, miR-345-3p regulated cell apoptosis through the TAK1/P38/NF-κB pathway by targeting *TRAF6* [23]. Interestingly, miR-146 regulated various biochemical processes by targeting *TRAF6*, including ameliorated HFD-induced non-alcoholic steatohepatitis [24] and reducing IL-1β-induced inflammatory factors in osteoblast-derived cell lines [25]. However, it remains unknown whether *TRAF6* plays a role as a miRNA target in adipogenic differentiation of intramuscular preadipocytes.

In this study, based on miRNA sequencing analysis of adipose tissue at four developmental stages of pigs at 1, 30, 90 and 240 days of age [26], we found that miR-146a-5p showed significant expression differences, implying it may have a key effect on IMF deposition. Our results revealed that miR-146a-5p inhibited the proliferation and differentiation of intramuscular preadipocytes by targeting *SMAD4* and *TRAF6* through TGF-β and NF-κB signal pathways, hinting that it is a novel key regulator in pig IMF deposition.

Methods

Animal and sample collection

Piglets (3 days) were provided by the animal experiment animal ranch of Northwest A&F University. According to the regulations of the Animal Protection Committee of Northwest A&F University, all pigs were killed in the slaughterhouse. Dissect the heart, liver, spleen, lung, kidney, dorsal longest muscle (LD) and subcutaneous white adipose tissue (SWAT), and rinse with phosphate buffered saline (PBS). The samples used for real-time quantitative PCR (RT-qPCR) were frozen and stored in liquid nitrogen.

Isolation and culture of porcine intramuscular preadipocytes

After the 3 days old piglets were sacrificed, the intramuscular preadipocytes in LD were extracted. Refer to this document for the specific operation method [27].

Transfection of mimics/inhibitor NC and miR-146a-5p mimic/inhibitor

Porcine intramuscular preadipocytes were seeded in 6-well, 12-well, 24-well or 96-well plates. When detecting cell proliferation, miR-146a-5p mimics or mimics negative control (MNC) (Ribobio, China) were transfected (50 nM) when the cell density reached 50–60%. During transfection, X-tremeGENE siRNA Transfection Reagent (Roche, USA) was mixed with Opti-MEM medium (Gibco, USA) for 5 minutes, then the two mixtures were mixed for 20 minutes and added to the cell culture medium, and the medium was replaced with fresh culture after 12 hours. Cells were harvested 24 hours after transfection for cell proliferation studies. When transfected with miR-146a-5p inhibitor, the method is the same as above, but the final concentration of miR-146a-5p inhibitor was 100 nM. For the differentiation of preadipocytes, the cells are transfected when the cell density reaches 70%. When cells grow to confluence after transfection, adipogenic differentiation begins by switching to differentiation medium.

Total RNA extraction, RNA reverse transcription and RT-qPCR

After obtaining the cells, the cells were lysed with Trizol reagent (TakaRa, Otsu, Japan) and the total RNA in the cells was extracted. The concentration of total RNA was measured by the NanoDrop 2000 (Thermo, Waltham, MA, USA). Then the reverse transcription kit (TakaRa, Otsu, Japan) was used to synthesize cDNA. The specific reverse transcription primers and procedures were used for miRNA inversion. About real-time quantitative PCR, the SYBR green kit was used and three replicates were set up, and then the PCR reaction was performed on the Bio-Rad iQTM5 system. GAPDH was used as the internal reference for all genes for standardized analysis. But when analyzing miR-146a-5p levels, U6 was used as an internal reference. Table 1 shows the primer sequences used for qPCR. The primer sequences used for qPCR were shown in Table 1.

Table 1
Primer sequences used in this study.

Gene	Forward (5'–3')	Reverse (5'–3')
Cyclin B	AATCCCTTCTTGTGGTTA	CTTAGATGTGGCATACTTG
Cyclin D	TACACCGACAACTCCATCCG	GAGGGCGGGTTGGAAATGAA
Cyclin E	CAGAGCAGCGAGCAGGAGC	GCAAGCTGCTTCCACACCACAT
P21	AGGTCGGAGTGAACGGATTTG	AGGTCGGAGTGAACGGATTTG
C/EBPβ	AGGTCGGAGTGAACGGATTTG	AGGTCGGAGTGAACGGATTTG
PPARγ	AGGTCGGAGTGAACGGATTTG	AGGTCGGAGTGAACGGATTTG
FABP4	AGGTCGGAGTGAACGGATTTG	AGGTCGGAGTGAACGGATTTG
SMAD4	TCACTATGAGCGGGTTGTCTC	TCCTTCAGTGGGTAAGGACG
TRAF6	GGGAACGATACGCCTTACAA	CTCTGTCTTAGGGCGTCCAG
GAPDH	AGGTCGGAGTGAACGGATTTG	AGGTCGGAGTGAACGGATTTG

Western blots

Cell samples were lysed using radio immunoprecipitation assay (RIPA) buffer (Beyotime, China) supplemented with protease inhibitor (Pierce, WA, USA) and total protein was extracted. The total protein samples were separated by electrophoresis in SDS-polyacrylamide gel. Then transferred it to PVDF membranes (Millipore, Bedford, MA, USA). After blocking the membrane in 5% skim milk for 2 hours, the primary antibody was incubated overnight (4 °C) and the secondary antibody was incubated for 1.5 hours (4 °C). Protein bands were exposed with chemiluminescent reagents (Millipore, Bedford, MA, USA) and quantified using Image J. Following primary antibodies were used: Cyclin D (1:100; Santa Cruz, USA), Cyclin E (1:100; Santa Cruz, USA), PCNA (1:1000; CST, USA), P21 (1:100; Santa Cruz, USA), C/EBPβ (1:100; Santa Cruz, USA), PPARγ(1:100; Santa Cruz, USA), FABP4 (1:100; Santa Cruz Biotechnology, Dallas, TX, USA), TRAF6 (1:500; Aviva Systems Biology, USA), SMAD4 (1:100; Santa Cruz, USA), β-actin (1:1000; Santa Cruz Biotechnology, Dallas, TX, USA), The secondary antibodies were anti-rabbit, anti-goat and anti-mouse antibodies (1:3000; Santa Cruz Biotechnology, Dallas, TX, USA). The targeted proteins were detected using the Gel Doc XR System (Bio-Rad, Hercules, CA, USA) as the instructions of the manufacturer.

Target prediction and luciferase activity assay

The target genes of miR-146a-5p were predicted with Target-Scan 7.0. For the dual-reporter assay, we constructed a wild-type and mutant psiCHECK-2-reporter vector containing the target genes SMAD4 and TRAF6 3' UTR region (TongYng). HEK293T was seeded in a 48-well plate and cotransfected with miRNA mimics or the negative control with psiCHECK-2–SMAD4 (or TRAF6)-reporter vector or mutant vector. After 48 h of transfection, the relative luciferase activity of Renilla compared with firefly was measured.

EDU imaging assay

We used the Cell-Light™ EdU Apollo® 567 In Vitro Imaging Kit and configured the mixed solution according to the instructions. The preadipocytes in the normal growth stage were treated with 50 μM EDU medium for 2 h. After the cells were fixed with 4% paraformaldehyde, they were stained with Apollo reaction solution. Then cell nucleus was stained with Hoechst. Nikon TE2000 microscope (Nikon, Tokyo, Japan) was used to take pictures, and the data was analyzed using Image J.

Cell Counting kit 8 (CCK8) analysis

Preadipocytes were seeded to 96-well plate in a number of 4×10^3 cells. Preadipocytes were transfected with miR-146a-5p mimics / inhibitor or mimics / inhibitor negative control with 3 repetitions. After treatment for 24 h we switched the cells to culture medium containing 10% CCK solution for 2 h at 37 °C followed by measuring absorbance at 490 nm.

Flow cytometry

After 24 hours of cell treatment, first wash 3 times with PBS, then fix the cells with 70% alcohol at -20 °C overnight, then treat with RNaseA at 37 °C (1 mg/mL, 40 min), and stained with propidium iodide (PI) at 4 °C (50 mg/mL, 1 h). The samples were detected using a FACS Calibur flow cytometer (Becton Dickinson, Franklin Lakes, NJ, USA). The proliferation index (PI) shows the proportion of mitotic cells among the 10,000 cells examined.

Oil Red O, BODIPY and AdipoRed staining

For Oil Red O staining, cells were fixed in a 4% paraformaldehyde solution for 30 minutes, induced with 60% Oil Red O for 30 minutes, and washed three times with PBS, and then the cells were visualized by phase-contrast microscope (IS-Elements software, Nikon ECLIPSE, Tokyo, Japan). Oil Red O was extracted with 100% isopropanol, and its relative concentration was determined by measuring the absorbance at 510 nm. After being fixed in 4% paraformaldehyde solution for 15 min, cells were stained with BODITY (1 μg/mL; Life Technologies, Carlsbad, CA, USA) or AdiopRed (30 μl / ml; Lonza, USA) for 20 min; the sections were washed with PBS three times for 5 min each. For nuclear visualization, DAPI

(4',6-diamidino-2-phenylindole; Roche) was incubated for 10 min, then the section was rinsed with PBS. After treatment, the sections were observed under fluorescence microscope (Nikon, Tokyo, Japan).

Bioinformatics analysis

The sequences of miRNAs were searched for at miRBase (http://www. mirbase.org/). Sequence alignment using MAGA software. The 3'UTR sequences of E2F3 and P55PIK were downloaded from NCBI. Target genes of miRNA were predicted by TargetScan 7.0 Human (http://www.targetscan.org).

Statistical analysis

All charts were created using GraphPad Prism 6.0 and the data represent the mean ± SEM. The significance of differences between the groups was assessed using the Student's t test or one-way analysis (*, *P*□0.05; **, p□0.01).

Results

MiR-146a-5p is a potential regulator in porcine IMF adipogenesis

To screen out miRNAs related to porcine IMF deposition, miRNA-sequencing data were analyzed. As shown in the heat map, the levels of miR-146a-5p of 30 d, 90 d, and 240 d porcine adipose tissue were significantly higher than that of 0 d piglets (Fig. 1A). Moreover, the seed sequence of miR-146a-5p in humans, pigs and mice is highly conserved (Fig. 1B). KEGG pathway analysis predicted that miR-146a-5p was involved in the TGF-β and NF-κB pathways (Fig. 1C), GO term analysis suggested that miR-146a-5p could regulate cell proliferation and fat cell differentiation (Fig. 1D). Furthermore, miR-146a-5p highly expressed in porcine WAT (Fig. 1E). Most importantly, the levels of miR-146a-5p increased first and then decreased in proliferated and differentiated porcine intramuscular preadipocytes, but they showed an upward trend in the late stage of differentiation (Fig. 1F and G).

MiR-146a-5p mimics inhibits proliferation of porcine intramuscular preadipocytes

To investigate the effect of miR-146a-5p on the proliferation of porcine intramuscular preadipocytes, the miR-146a-5p mimics and mimics negative control (MNC) were transfected into cells. Compared with the MNC group, the positive cells labeled with EDU and total number of cells in the mimics group significantly reduced ($P < 0.05$) (Fig. 2A-C). In addition, the number of S-phase cells in mimics group was significantly less than MNC group ($P < 0.05$), but the number of cells in the G1-phase was significantly more than MNC group ($P < 0.05$) (Fig. 2D and E). Furthermore, the miR-146a-5p mimics sharply increased the level of miR-

146a-5p ($P < 0.05$), significantly decreased the mRNA levels of *cyclin B*, *cyclin D* and *cyclin E*, whereas apparently increased the mRNA levels of *P21* ($P < 0.05$) (Fig. 2F and G). Similarly, the miR-146a-5p mimics downregulated the protein levels of cyclin D, cyclin E and PCNA ($P < 0.05$), and P21 protein tended to upregulated, but not reach statistical significance (Fig. 2H and I).

MiR-146a-5p inhibitor promotes porcine intramuscular preadipocyte proliferation

To validate the role of miR-146a-5p inhibitor on the proliferation of porcine intramuscular preadipocytes, inhibitor negative control (INC) and miR-146a-5p inhibitors were transfected into porcine intramuscular preadipocytes. The results indicated that knockdown of miR-146a-5p significantly increased the number of EDU positive cells, S - phase cells and the total cells ($P < 0.05$) (Fig. 3A-E). The inhibitor effectively decreased the levels of miR-146a-5p ($P < 0.05$), and increased the mRNA levels of *cyclin B*, *cyclin D* and *cyclin E*, but reducing the level of *P21* ($P < 0.05$) (Fig. 3F and G). Meanwhile inhibitor upregulated the protein levels of cyclin D and cyclin E, whereas downregulated the protein level of P21 ($P < 0.05$) (Fig. 3H and I).

MiR-146a-5p targeting SMAD4 inhibits the proliferation of porcine intramuscular preadipocytes by TGF-β signaling pathway

To further explore the regulatory mechanism of miR-146a-5p on porcine intramuscular preadipocyte proliferation, we predicted and verified its target genes and signaling pathway. *SMAD4* may be the target gene of miR-146a-5p using TargetScan 7.0 analysis (Fig. 4A and B). The dual-luciferase reporter (DLR) assay results showed that the relative luciferase activity of miR-146a-5p mimics plus *SMAD4* WT vector co-treated group significantly reduced ($P < 0.05$) (Fig. 4C and D). Next, the rescued experiments were further carried out. Compared with the mimics group, the number of EDU-positive cells and the total cells numbers in the mimics and *SMAD4* overexpression vector co-treatment group markedly increased ($P < 0.01$), and rescued or even exceeded the NC group level (Fig. 4E-G). Moreover, *SMAD4* overexpression restored the mRNA and protein levels of *SMAD4* and cell cycle-related genes ($P < 0.05$) (Fig. 4H-K). In addition, the SMAD4 downstream TGF-β signaling was attenuated by mimics, but was rescued when *SMAD4* overexpression ($P < 0.05$) (Fig. 4J and K).

MiR-146a-5p mimics suppresses porcine intramuscular preadipocyte differentiation

To study the effects of miR-146a-5p mimics on the differentiation of porcine intramuscular preadipocytes, we treated cells with MNC and miR-146a-5p mimics, then induced adipogenic differentiation for 6 days. Compared with the MNC group, the lipid droplets produced by intramuscular adipocytes apparently decreased in mimics group, and the triglycerides (TG) content also significantly

decreased ($P < 0.05$) (Fig. 5A-D). The expression of miR-146a-5p was significantly increased in differentiated intramuscular adipocytes ($P < 0.05$) (Fig. 5E). Similarly, the mRNA and protein levels of *C/EBPβ*,*PPARγ* and *FABP4* ($P < 0.05$) (Fig. 5F-H).

MiR-146a-5p inhibitor accelerates porcine intramuscular preadipocyte differentiation

To further validate the role of miR-146a-5p in the differentiation of porcine intramuscular preadipocytes, we carried out the experiments of INC and inhibitor treatment on the cells. Compared with the INC group, the lipid droplets apparently accumulated in intramuscular adipocytes, and the TG content also significantly increased ($P < 0.05$) (Fig. 6A-D). Inhibitors significantly decreased the level of miR-146a-5p (Fig. 6E), but markedly increased the mRNA levels of *C/EBPβ*, *PPARγ* and *FABP4* ($P < 0.05$) (Fig. 6F). Meanwhile the protein levels of C/EBPβ and PPARγ significantly increased in the treatment group ($P < 0.05$) (Fig. 6G and H).

MiR-146a-5p targeting TRAF6 inhibits the differentiation of porcine intramuscular preadipocytes via NF-κB signaling pathway

To further investigate the mechanism by which miR-146a-5p regulates the differentiation of intramuscular preadipocytes, we explored its target genes and signaling pathways. Online software predicted that miR-146a-5p could be combined with *TRAF6* 3'UTR (Fig. 7A and B). The DLR assay result showed that the relative luciferase activity of miR-146a-5p mimics and *TRAF6* WT vector co-treated group was significantly reduced ($P < 0.05$) (Fig. 7C and D). The rescued experiments were further performed. Compared with the mimics group, the lipid droplets and TG content in the *TRAF6* overexpression vector plus mimics co-treated group significantly increased and rescued to the NC group level ($P < 0.05$) (Fig. 7E-H). Moreover, *TRAF6* overexpression rescued the mRNA and protein levels of *TRAF6* and adipogenic related genes ($P < 0.05$) (Fig. 7I-L). NF-κB as an important one of TRAF6 downstream signaling molecules, the levels of NF-κB and its phosphorylation levels were significantly decreased in mimics group but increased in co-treated group ($P < 0.01$) (Fig. 7M and N).

Discussion

As a member of the non-coding RNA family, miRNA has a crucial regulatory role in preadipocyte adipogenesis. Based on bioinformatics analysis of miRNAs sequencing data, we found that miR-146a-5p was differentially expressed during SWAT deposition in pigs. Further study showed that the miR-146a-5p sequence was highly conserved, and its function was involved in fat cell proliferation and differentiation by TGF-β and NF-κB signal pathways using KEGG and GO analysis. Moreover, miR-146a-5p not only highly expressed in porcine WAT, but also its expression levels increased first and then decreased in proliferated and differentiated porcine intramuscular preadipocytes. Based on above analysis, we therefore speculated that miR-146a-5p also was implicated in IMF deposition.

It is a vital task to improve pork quality via control IMF content in pig production. The present study demonstrated that miR-146a-5p played a crucial role in regulating porcine IMF adipogenesis. MiR-146a-5p targeting *SMAD4* inhibited the proliferation of porcine intramuscular preadipocytes through attenuating TGF-β signaling, whereas it targeting *TRAF6* repressed differentiation by weakening NF-κB signaling. These findings indicated that miR-146a-5p could be a novel negative regulator of porcine IMF deposition.

The IMF deposition depended on the proliferation and differentiation of intramuscular preadipocytes. Our results confirmed that miR-146a-5p inhibited the proliferation of intramuscular preadipocytes by reducing the number of S-phase cells and downregulating the mRNA and protein levels of *cyclin B, cyclin D, cyclin E, PCNA* and upregulating the mRNA and protein levels of *P21*. Previous studies revealed that miR-146a-5p promotes lung cancer cells proliferation by targeting claudin-12 [28], and overexpression of miR-146 or knockout of its target gene notch 1 inhibited the proliferation of mouse neural stem cells under serum-free medium [29]. Therefore, miR-146a-5p discrepantly modulated proliferation in different types of cells. Generally, a gene or miRNA has the opposite effect on cell proliferation and differentiation. Recent studies showed that miR-664-5p promoted myoblast proliferation and inhibited myoblast differentiation [30], and miR-429 accelerated proliferation of porcine preadipocytes and repressed adipogenic differentiation [31]. Interestingly, in this study, miR-146a-5p repressed both proliferation and differentiation of intramuscular preadipocytes. Literatures indicated that miR-483 inhibited both the proliferation and differentiation of bovine myoblasts [32], as well as miR-342-5p restricted the proliferation and differentiation of osteoblasts by inhibiting the expression of Bmp7 [33]. Therefore, our results were reasonable because of complexity of the biological processes of intramuscular preadipocytes via miRNA regulation.

Generally, miRNAs regulate different biological processes in the same cell by different target genes. Therefore, we predicted the target genes of miR-146a-5p in cell proliferation and adipogenic differentiation, respectively. During the proliferation phase, we predicted that *SMAD4* was the target gene of miR-146a-5p. Recent studies showed that miR-145-5p inhibited the proliferation of ovarian epithelial cancer cells by targeting *SMAD4* [34], and the overexpression of miR-663a suppressed the hepatic stellate cell proliferation by downregulating *SMAD4* level [35]. Based on above results, *SMAD4* is mostly a positive regulator of cell proliferation. Moreover, The *SMAD4* and TGF-β signaling pathways played important roles in the process of miRNA regulating cell proliferation, respectively [36, 37]. Here, we revealed that miR-146a-5p targeting the *SMAD4* was identified as a novel miRNA that repressed proliferation of porcine intramuscular preadipocytes via the TGF-β signaling pathway.

Furthermore, we confirmed that the target gene of miR-146a-5p was *TRAF6* during adipogenic differentiation of porcine intramuscular preadipocytes through TargetScan 7.0 analysis, luciferase activity assay and rescued experiments. TRAF6 is a signal transduction factor that connects cell surface receptors with intracellular signal proteins. In addition to the inflammatory immune response, *TRAF6* also regulated cell differentiation and survival [38]. Previous studies showed that inhibiting the CD40-TRAF6 interaction treated obesity by improving glucose tolerance and reducing the accumulation of immune cells into adipose tissue [39]. Moreover, green tea extracts reduced the adipose tissue weight of obese

mice by reducing the expression of *TRAF6* [40]. Therefore, *TRAF6* has a positive regulatory effect on fat accumulation. Importantly, the NF-κB signaling which was the TRAF6 downstream inhibited inflammatory injury, promoted chondrocyte apoptosis and repressing pancreatic cancer cell proliferation [24, 41, 42]. In this study, we uncovered that miR-146a-5p targeting *TRAF6* inhibited differentiation of porcine intramuscular preadipocytes by NF-κB signaling pathway.

Conclusions

In conclusion, miR-146a-5p targeting *SMAD4* inhibited the proliferation of porcine intramuscular preadipocytes through TGF-β signal pathway, whereas targeting *TRAF6* repressed adipogenic differentiation via NF-κB signal pathway (Fig. 8). These findings not only provide a novel miRNA biomarker to modulate IMF content for promoting pork quality, but also help us to better understand the role and regulatory mechanism of miRNAs on IMF adipogenesis.

Abbreviations

IMF: Intramuscular fat; MiRNAs: MicroRNAs; SMAD4: SMAD family member 4; TRAF6: TNF receptor associated factor 6; WAT: White adipose tissue; CDKs: Cyclin-dependent kinases; CKIs: CDK inhibitors; PPARγ: Peroxisome proliferator-activated receptor γ; C/EBP: CCAAT / enhancer binding protein; FABP4: Fatty acid binding protein 4; LPL: Lipoprotein lipase; LD: longissimus dorsi; SWAT: subcutaneous white adipose tissue; PBS: Phosphate buffer saline; RT-qPCR: Real-time quantitative PCR; MNC: Mimics negative control; INC: Inhibitor negative control; DLR: Dual-luciferase reporter; TG: Triglycerides.

Declarations

Acknowledgments

We thank all the numbers of the Animal Fat Deposition and Muscle Development Laboratory of the College of Animal Science and Technology, Northwest A&F University who make efforts to these experiments. Zhang Que especially wishes to thank the support and encouragement of Ren Fa.

Authors’ contributions

Zhang Que, Cai Rui, Tang Guorong, Zhang Wanrong conducted the experiment; Zhang Que and Cai Rui collected and analyzed the data; Tang Guorong, Zhang Wanrong, and Pang Weijun helped with the discussion; Zhang Que, Cai Rui and Pang Weijun designed the experiment; Zhang Que, Cai Rui and Pang Weijun wrote and revised the manuscript; The authors read and approved the final manuscript.

Funding

This work was supported by grants from the National Natural Science Foundation (31872979, 31572366), the National Key Research and Development Program of China (2017YFD0502002), and the National Basic Research Programs of China (2015CB943102).

Availability of data and materials

All data generated or analyzed during this study are available from the corresponding author by request.

Ethics approval and consent to participate

All experimental procedures were performed according to the Guide for Northwest A&F University Animal Care Committee. The experimental protocol was approved by the Departmental Animal Ethics Committee of Northwest A&F University (14-233, 10 December 2014). As suggested by the animal welfare protocol, all efforts were made to reduce animal suffering and to use only the number of animals required to produce dependable scientific data.

Consent for publication

Not applicable.

Competing interests

The authors have declared no conflict of interest.

References

1. Fernandez X, Monin G, Talmant A, Mourot J, Lebret B. Influence of intramuscular fat content on the quality of pig meat - 1. Composition of the lipid fraction and sensory characteristics of m. longissimus lumborum. Meat Sci. 1999;53(1):59-65.
2. Nogalski Z, Pogorzelska-Przybyłek P, Białobrzewski I, Modzelewska-Kapituła M, Sobczuk-Szul M, Purwin C. Estimation of the intramuscular fat content of m. longissimus thoracis in crossbred beef cattle based on live animal measurements. Meat Sci. 2017;125:121-27.
3. Chen L, Zhang Y, Chen H, Zhang X, Liu X, He Z, et al. Comparative Transcriptome Analysis Reveals a More Complicated Adipogenic Process in Intramuscular Stem Cells than That of Subcutaneous Vascular Stem Cells. J Agric Food Chem. 2019;67(16):4700-8.
4. Petrus P, Mejhert N, Corrales P, Lecoutre S, Li Q, Maldonado E, et al. Transforming Growth Factor-β3 Regulates Adipocyte Number in Subcutaneous White Adipose Tissue. Cell Rep. 2018;25(3):551-60.e5.

5. Sun Y, Cai R, Wang Y, Zhao R, Qin J, Pang W. A Newly Identified LncRNA LncIMF4 Controls Adipogenesis of Porcine Intramuscular Preadipocyte through Attenuating Autophagy to Inhibit Lipolysis. Animals (Basel). 2020;10(6):E926.
6. Nobre JL, Lisboa PC, Carvalho JC, Martins MR, Vargas S, Barja-Fidalgo C, et al. Leptin blocks the inhibitory effect of vitamin D on adipogenesis and cell proliferation in 3T3-L1 adipocytes. Gen Comp Endocrinol. 2018;266:1-8.
7. Lujambio A, Lowe SW. The microcosmos of cancer. Nature. 2012;482(7385):347-55.
8. Maurizi G, Babini L, Della Guardia L. Potential role of microRNAs in the regulation of adipocytes liposecretion and adipose tissue physiology. J Cell Physiol. 2018;233(12):9077-86.
9. Xu K, Ji M, Huang X, Peng Y, Wu W, Zhang J. Differential Regulatory Roles of MicroRNAs in Porcine Intramuscular and Subcutaneous Adipocytes. J Agric Food Chem. 2020;68(13):3954-62.
10. Khan R, Raza SHA, Junjvlieke Z, Wang X, Wang H, Cheng G, et al. Bta-miR-149-5p inhibits proliferation and differentiation of bovine adipocytes through targeting CRTCs at both transcriptional and posttranscriptional levels. J Cell Physiol. 2020;235(7-8):5796-810.
11. Du J, Zhang P, Gan M, Zhao X, Xu Y, Li Q, et al. MicroRNA-204-5p regulates 3T3-L1 preadipocyte proliferation, apoptosis and differentiation. Gene. 2018;668:1-7.
12. Xing K, Zhao X, Ao H, Chen S, Yang T, Tan Z, et al. Transcriptome analysis of miRNA and mRNA in the livers of pigs with highly diverged backfat thickness. Sci Rep. 2019;9(1):16740.
13. Mohd Faheem M, Rasool RU, Ahmad SM, Jamwal VL, Chakraborty S, Katoch A, et al. Par-4 mediated Smad4 induction in PDAC cells restores canonical TGF-beta / Smad4 axis driving the cells towards lethal EMT. Eur J Cell Biol. 2020;99(4):151076.
14. Massagué J, Gomis RR. The logic of TGFbeta signaling. FEBS Lett. 2006;580(12):2811-20.
15. Zhao M, Mishra L, Deng CX. The role of TGF-beta/SMAD4 signaling in cancer. Int J Biol Sci. 2018;14(2):111-23.
16. Wan R, Xu X, Ma L, Chen Y, Tang L, Feng J. Novel Alternatively Spliced Variants of Smad4 Expressed in TGF-β-Induced EMT Regulating Proliferation and Migration of A549 Cells. Onco Targets Ther. 2020;13:2203-13.
17. Zuo Y, Lu Y, Xu Q, Sun D, Liang X, Li X, et al. Inhibitory effect of dihydromyricetin on the proliferation of JAR cells and its mechanism of action. Oncol Lett. 2020;20(1):357-63.
18. Zhou J, Hu M, Wang F, Song M, Huang Q, Ge B. miR-224 Controls Human Colorectal Cancer Cell Line HCT116 Proliferation by Targeting Smad4. Int J Med Sci. 2017;14(10):937-42.
19. Fu TM, Shen C, Li Q, Zhang P, Wu H. Mechanism of ubiquitin transfer promoted by TRAF6. Proc Natl Acad Sci U S A. 2018;115(8):1783-88.
20. Jeong S, Cho IR, An WG, Jhun BH, Lee BS, Park K, et al. STP-A11, an oncoprotein of Herpesvirus saimiri augments both NF-κB and AP-1 transcription activity through TRAF6. Experimental & Molecular Medicine. 2007;39(1):56-64.

21. Jiang WW, Gao LL, Ming WU, Zhao T, Shen DL. Effect of lipoxin A4 on the expression of Toll-like receptor 4 and TNF receptorassociated factor 6 in the liver of obese rats with sepsis. Chinese Journal of Contemporary Pediatrics. 2018;20(7):578-84.
22. Kim HS, Han SY, Sung HY, Park SH, Kang MK, Han SJ, et al. Blockade of visfatin induction by oleanolic acid via disturbing IL-6-TRAF6-NF-κB signaling of adipocytes. Exp Biol Med. 2014;239(3):284-92.
23. Wei Q, Tu Y, Zuo L, Zhao J, Chang Z, Zou Y, et al. MiR-345-3p attenuates apoptosis and inflammation caused by oxidized low-density lipoprotein by targeting TRAF6 via TAK1/p38/NF-kB signaling in endothelial cells. Life Sci. 2020;241:117142.
24. Jiang W, Liu J, Dai Y, Zhou N, Ji C, Li X. MiR-146b attenuates high-fat diet-induced non-alcoholic steatohepatitis in mice. J Gastroenterol Hepatol. 2015;30(5):933-43.
25. Pan J, Du M, Cao Z, Zhang C, Hao Y, Zhu J, et al. miR-146a-5p attenuates IL-1beta-induced IL-6 and IL-1beta expression in a cementoblast-derived cell line. Oral Dis. 2020. https://doi.org/10.1111/odi.13333.
26. Wang Q, Qi R, Wang J, Huang W, Wu Y, Huang X, et al. Differential expression profile of miRNAs in porcine muscle and adipose tissue during development. Gene. 2017;618:49-56.
27. Chen FF, Xiong Y, Peng Y, Gao Y, Qin J, Chu GY, et al. miR-425-5p Inhibits Differentiation and Proliferation in Porcine Intramuscular Preadipocytes. Int J Mol Sci. 2017;18(10):2101.
28. Sun X, Cui S, Fu X, Liu C, Wang Z, Liu Y. MicroRNA-146-5p promotes proliferation, migration and invasion in lung cancer cells by targeting claudin-12. Cancer Biomark. 2019;25(1):89-99.
29. Xiao WZ, Lu AQ, Liu XW, Li Z, Zi Y, Wang ZW. Role of miRNA-146 in proliferation and differentiation of mouse neural stem cells. Biosci Rep. 2015;35(5):e00245.
30. Cai R, Qimuge N, Ma ML, Wang YQ, Tang GR, Zhang Q, et al. MicroRNA-664-5p promotes myoblast proliferation and inhibits myoblast differentiation by targeting serum response factor and Wnt1. J Biol Chem. 2018;293(50):19177-90.
31. Peng Y, Chen FF, Ge J, Zhu JY, Shi XE, Li X, et al. miR-429 Inhibits Differentiation and Promotes Proliferation in Porcine Preadipocytes. Int J Mol Sci. 2016;17(12):2047.
32. Song CC, Yang ZX, Dong D, Xu JW, Wang J, Li H, et al. miR-483 inhibits bovine myoblast cell proliferation and differentiation via IGF1/PI3K/AKT signal pathway. J Cell Physiol. 2019;234(6):9839-48.
33. Li X, Li K, Yu G, Yu C, Liu C. miR-342-5p inhibits expression of Bmp7 to regulate proliferation, differentiation and migration of osteoblasts. Mol Immunol. 2019;114:251-9.
34. Zhou J, Zhang X, Li W, Chen Y. MicroRNA-145-5p regulates the proliferation of epithelial ovarian cancer cells via targeting SMAD4. J Ovarian Res. 2020;13(1):54.
35. Guo XX, Yang WN, Dong BS, Shang JW, Su SB, Yan XL, et al. Glycyrrhetinic Acid-Induced MiR-663a Alleviates Hepatic Stellate Cell Activation by Attenuating the TGF-β/Smad Signaling Pathway. Evid Based Complement Alternat Med. 2020;2020:3156267.

36. Zhang Z, Wang W, Liu JB, Wang Y, Hao JD, Huang YJ, et al. ssc-miR-204 regulates porcine preadipocyte differentiation and apoptosis by targeting TGFBR1 and TGFBR2. J Cell Biochem. 2020;121(1):609-20.
37. Stewart A, Guan HY, Yang KP. BMP-3 Promotes Mesenchymal Stem Cell Proliferation Through the TGF-beta/Activin Signaling Pathway. Journal of Cellular Physiology. 2010;223(3):658-66.
38. Walsh MC, Lee J, Choi Y. Tumor necrosis factor receptor- associated factor 6 (TRAF6) regulation of development, function, and homeostasis of the immune system. Immunol Rev 2015;266(1):72-92.
39. Van den Berg SM, Seijkens TT, Kusters PJ, Zarzycka B, Beckers L, den Toom M, et al. Blocking CD40-TRAF6 interactions by small-molecule inhibitor 6860766 ameliorates the complications of diet-induced obesity in mice. Int J Obes (Lond). 2015;39(5):782-90.
40. Cunha CA, Lira FS, Rosa Neto JC, Pimentel GD, Souza GI, da Silva CM, et al. Green tea extract supplementation induces the lipolytic pathway, attenuates obesity, and reduces low-grade inflammation in mice fed a high-fat diet. Mediators Inflamm. 2013;2013:635470.
41. Ge YT, Zhong AQ, Xu GF, Lu Y. Resveratrol protects BV2 mouse microglial cells against LPS-induced inflammatory injury by altering the miR-146a-5p/TRAF6/NF-kappaB axis. Immunopharmacol Immunotoxicol. 2019;41(5):549-57.
42. Shao J, Ding Z, Peng J, Zhou R, Chen Y. MiR-146a-5p promotes IL-1β-induced chondrocyte apoptosis through the TRAF6-mediated NF-kB pathway. Inflammation Research. 2020;69(6):619-30.

Figures

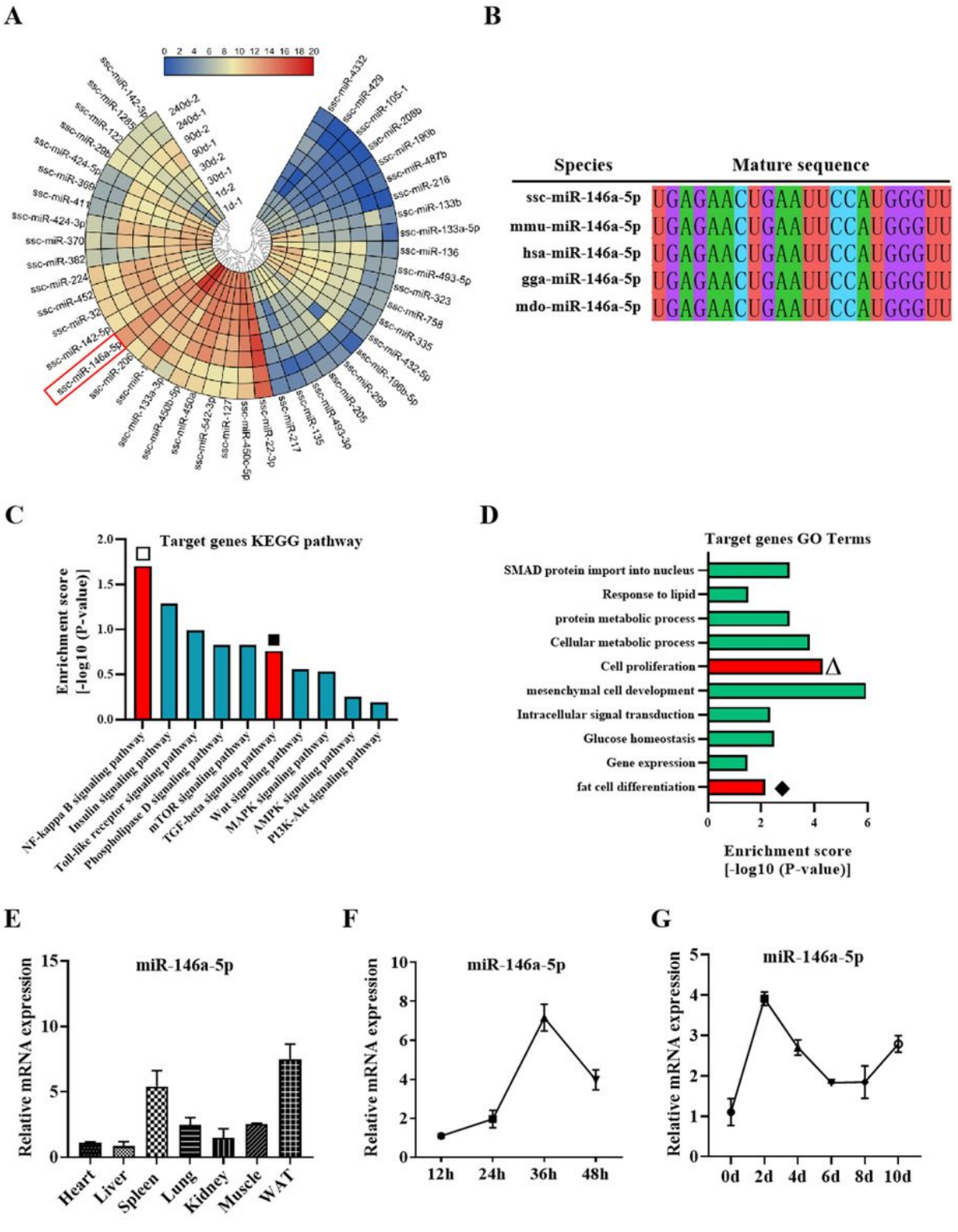

Figure 1

MiR-146a-5p is a potential regulator in porcine IMF adipogenesis. A, the differential expression analysis heat map of miRNA sequencing data. Different colors represented the relative expression. B, comparation of miR-146a-5p seed sequence from pig, mice and human et al. C, KEGG pathway analysis of the miR-146a-5p target genes. D, GO term analysis of the miR-146a-5p target genes. E, tissue expression profile of miR-146a-5p in pig. F, RT-qPCR was performed to detect the expression of miR-146a-5p in proliferating in

porcine intramuscular preadipocytes. G, RT-qPCR analysis of miR-146a-5p expression after inducing adipogenic differentiation. Results are representative of the mean ± S.E.M (n=3).

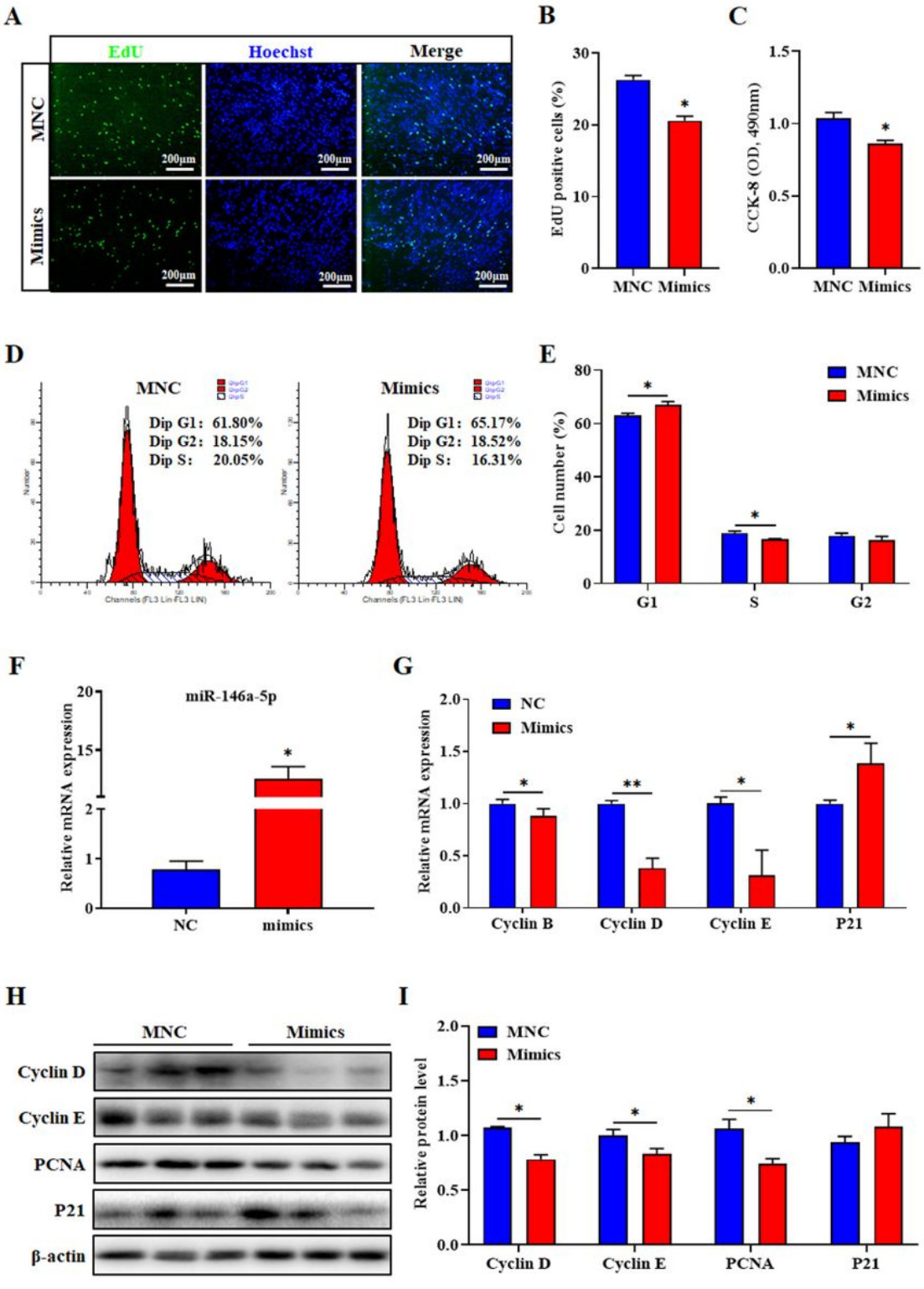

Figure 2

MiR-146a-5p mimics inhibits proliferation of porcine intramuscular preadipocytes. A, EdU staining assay. Porcine intramuscular preadipocyte in the S-phase were stained with EdU in red, and cell nuclei were dyed with Hoechst in blue. B, quantification ratio of EdU-positive cells/total cells. C, CCK-8 analysis after

treatment with miR-146a-5p mimics during porcine intramuscular preadipocyte proliferation. D, cell cycle analysis of preadipocyte by flow cytometry. E, statistical results of flow cytometry. F, overexpression efficiency of miR-146a-5p mimics after transfection for 24 h. G, RT-qPCR was used to detect the cell cycle genes cyclin B,cyclin D, cyclin E, and p21. H, western blot analysis of cyclin E, cyclin D, PCNA and p21 after transfection with miR-146a-5p mimics. I, protein quantitative analysis of cyclin E, cyclin D, PCNA and p21. Values are expressed as mean ± S.E.M (n = 3). *, $p < 0.05$; **, $p < 0.01$, versus MNC.

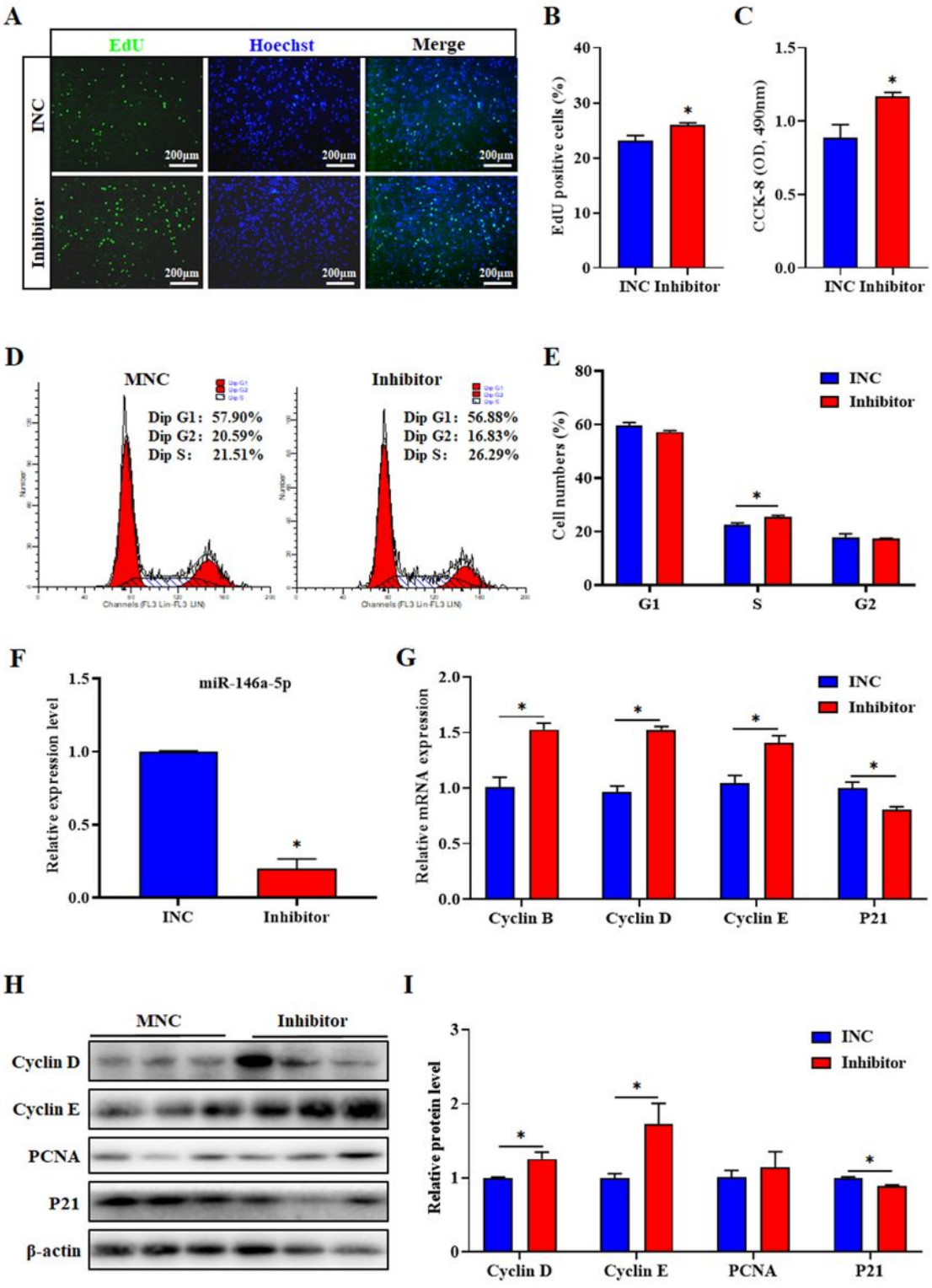

Figure 3

MiR-146a-5p inhibitor promotes porcine intramuscular preadipocyte proliferation. A, EdU staining assay. Porcine intramuscular preadipocyte in the S-phase were stained with EdU in red, and cell nuclei were dyed with Hoechst in blue. B, quantification ratio of EdU-positive cells/total cells. C, CCK-8 analysis after treatment with miR-146a-5p inhibitor during porcine intramuscular preadipocyte proliferation. D, cell cycle analysis of preadipocyte by flow cytometry. E, statistical results of flow cytometry. F, interference efficiency of miR-146a-5p inhibitor after transfection for 24 h. G, RT-qPCR was used to detect the cell cycle genes cyclin B,cyclin D, cyclin E, and p21. H, Western blot analysis of cyclin E, cyclin D, PCNA and p21 after transfection with miR-146a-5p inhibitor. I, protein quantitative analysis of cyclin E, cyclin D, PCNA and p21. Values are expressed as the mean ± S.E.M (n = 3). *, $p < 0.05$, versus INC.

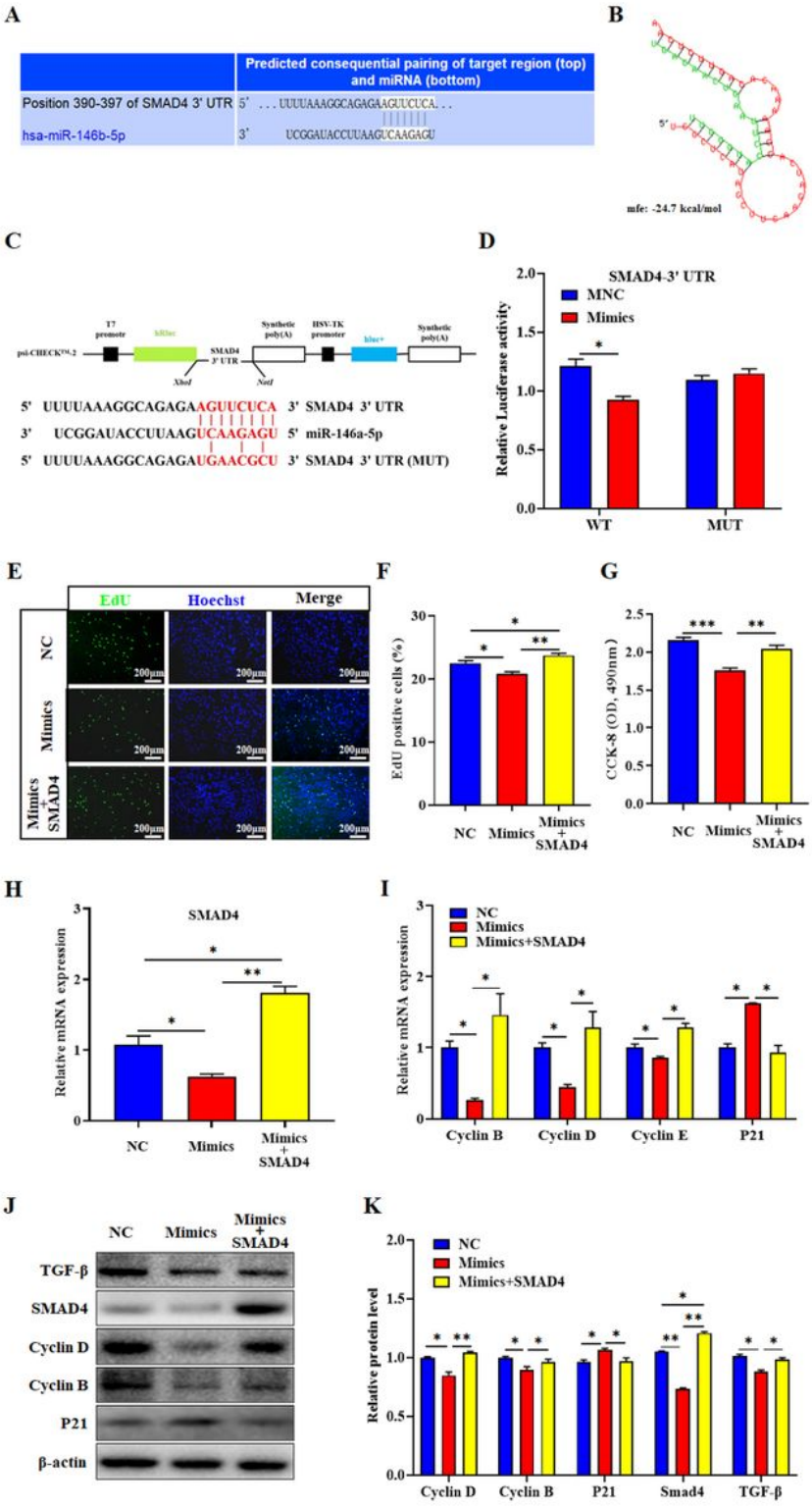

Figure 4

MiR-146a-5p targeting SMAD4 inhibits the proliferation of porcine intramuscular preadipocytes by TGF-β signaling pathway. A, SMAD4 was predicted to be a target of miR-146a-5p by TargetScan software. B, miR-146a-5p and SMAD4 3'UTR region base complementary pattern diagram. C, WT and MUT psiCHECK-2.0-SMAD4 vectors. D, relative luciferase activity of SMAD4 responding to miR-146a-5p mimics. To verify that miR-146a-5p can function by targeting SMAD4, we co-treated cells with miR-146a-5p mimics and

SMAD4 overexpression vector (500ng, 6-well plate). E, EdU staining assay. F, quantification ratio of EdU-positive cells/total cells. G, CCK-8 analysis. H, RT-qPCR was used to detect SMAD4 mRNA expression level. I, cell cycle genes cyclin B,cyclin D, cyclin E, and p21 expression level. J, Western blot analysis of cyclin E, cyclin D, PCNA and p21. K, protein quantitative analysis of cyclin E, cyclin D, PCNA and p21. Values are expressed as the mean ± S.E.M. (n = 3). *, p < 0.05; **, p < 0.01; ***, p < 0.001, versus NC.

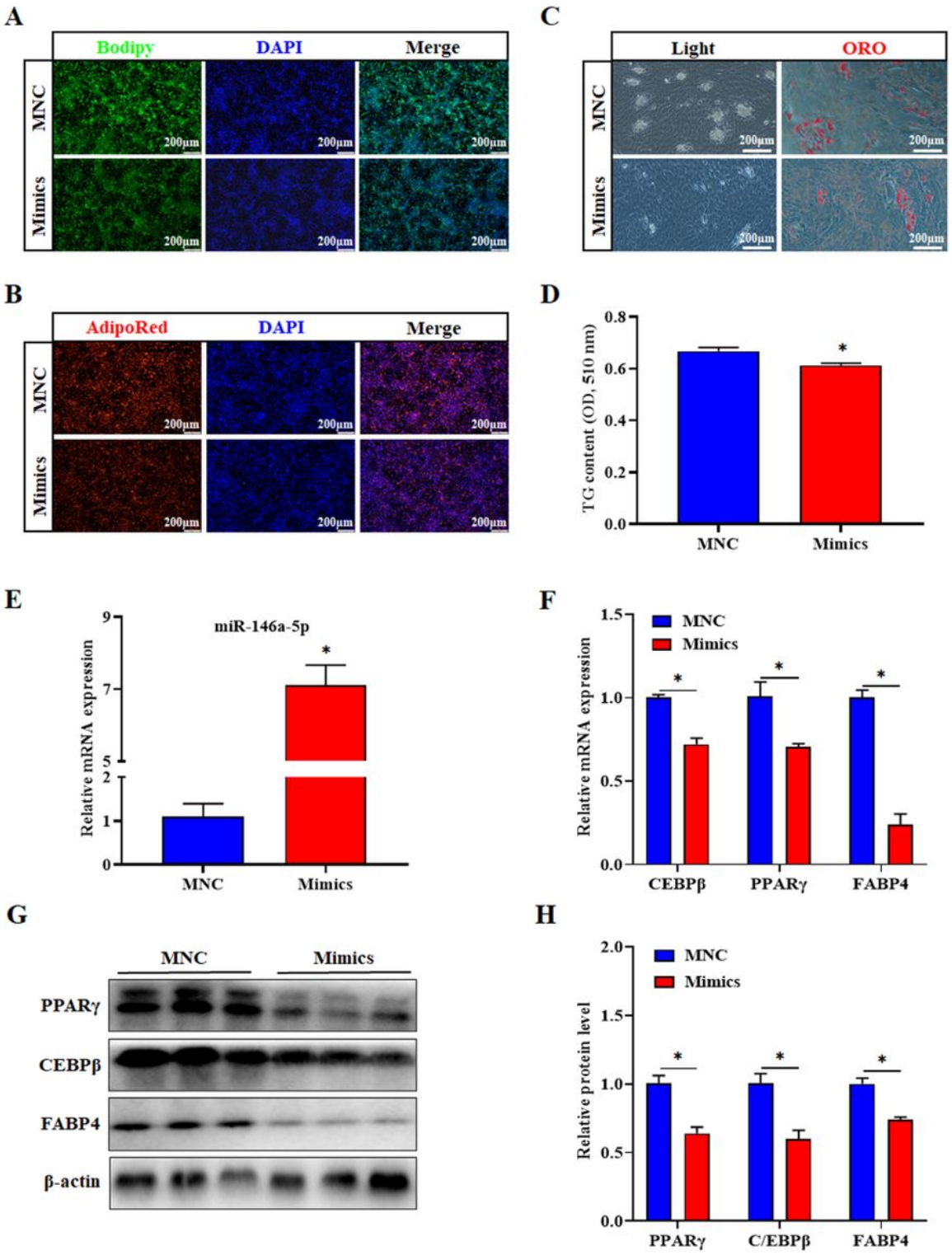

Figure 5

MiR-146a-5p mimics suppresses porcine intramuscular preadipocyte differentiation. Porcine intramuscular preadipocyte were treated with miR-146a-5p mimics to induce differentiation on the 6th day. A and B, Bodipy or AdipoRed staining was performed on lipid droplets. C, white light field and oil red O stained lipid droplets. D, after extracting oil red O with isopropanol, the OD value was detected, 510 nm. E, overexpression efficiency of miR-146a-5p mimics after transfection for 6d. F, RT-qPCR was used to detect the adipogenesis genes C/EBPβ, PPARγ, and FABP4. G, Western blot analysis of C/EBPβ, PPARγ, and FABP4 after transfection with miR-146a-5p mimics. H, protein quantitative analysis of G. Values are expressed as the mean ± S.E. (n = 3). *, $p < 0.05$, versus MNC.

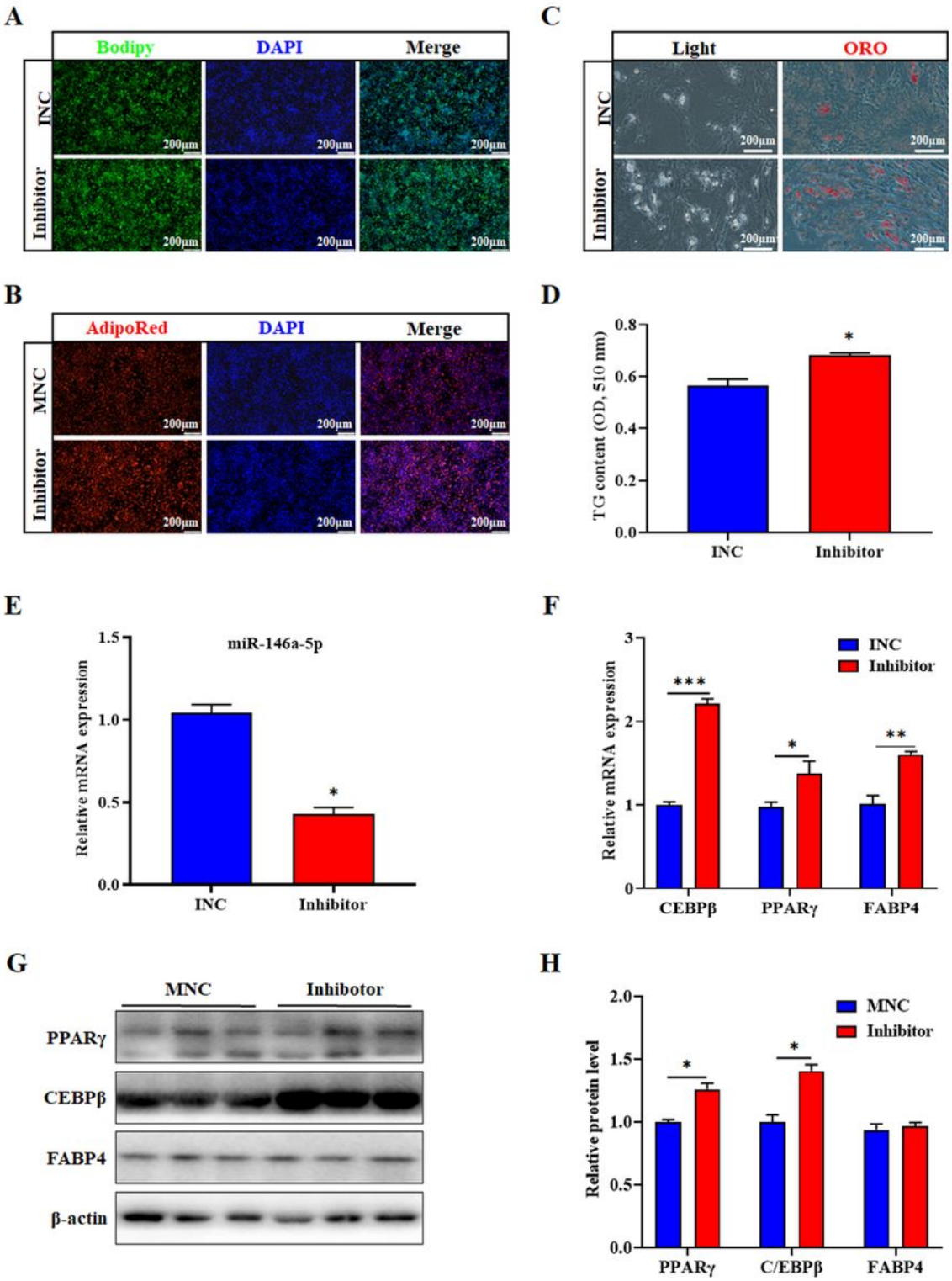

Figure 6

MiR-146a-5p inhibitor accelerates porcine intramuscular preadipocyte differentiation. A, Porcine intramuscular preadipocyte were treated with miR-146a-5p inhibitor to induce differentiation on the 6th day. A and B, Bodipy or AdipoRed staining was performed on lipid droplets. C, white light field and oil red O stained lipid droplets. D, after extracting oil red O with isopropanol, the OD value (510 nm) was detected. E, interference efficiency of miR-146a-5p inhibitor after transfection for 6d. F, RT-qPCR was used

to detect the adipogenesis genes C/EBPβ, PPARγ, and FABP4. G, Western blot analysis of C/EBPβ, PPARγ, and FABP4 after transfection with miR-146a-5p inhibitor. H, protein quantitative analysis of G. Values are expressed as the mean ± S.E. (n = 3). *, p < 0.05; **, p < 0.01, versus INC.

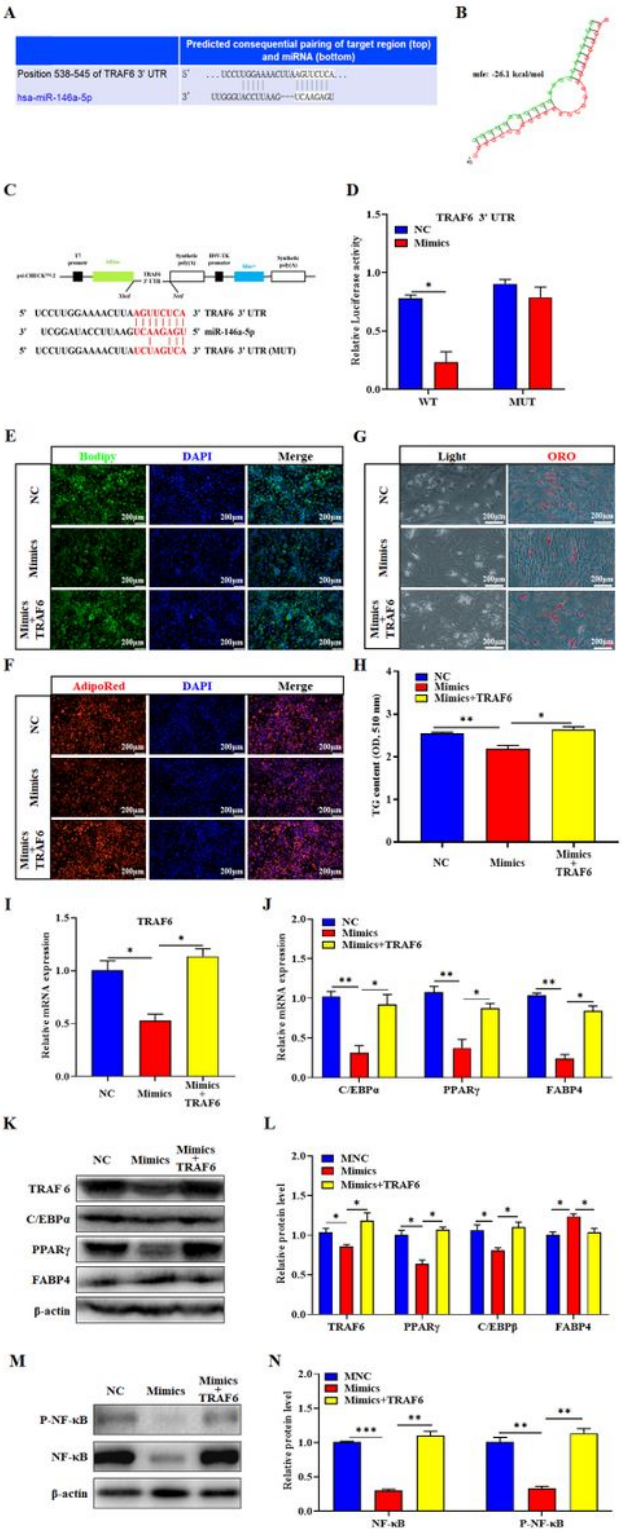

Figure 7

MiR-146a-5p targeting TRAF6 inhibits the differentiation of porcine intramuscular preadipocytes via NF-κB signaling pathway. A, TRAF6 was predicted to be a target of miR-146a-5p by TargetScan software. B,

miR-146a-5p and TRAF6 3' UTR region base complementary pattern diagram. C, WT and MUT psiCHECK-2.0-TRAF6 vectors. D, relative luciferase activity of TRAF6 responding to miR-146a-5p mimics. To verify that miR-146a-5p can function by targeting TRAF6, we co-treated cells with miR-146a-5p mimics and TRAF6 overexpression vector (500ng per hole, 6-well plate). E and F, Bodipy or AdipoRed staining was performed on lipid droplets. G, white light field and oil red O stained lipid droplets. H, after extracting oil red O with isopropanol, the OD value (510 nm) was detected. I and J, RT-qPCR was used to detect the TRAF6 and adipogenesis genes C/EBPβ, PPARγ, and FABP4. K, Western blot analysis of TRAF6, C/EBPβ, PPARγ, and FABP4. L, protein quantitative analysis of K. M, Western blot analysis of TRAF6, C/EBPβ, PPARγ, and FABP4. N, protein quantitative analysis of K. Values are expressed as the mean ± S.E. (n = 3). *, $p < 0.05$; **, $p < 0.01$, versus NC.

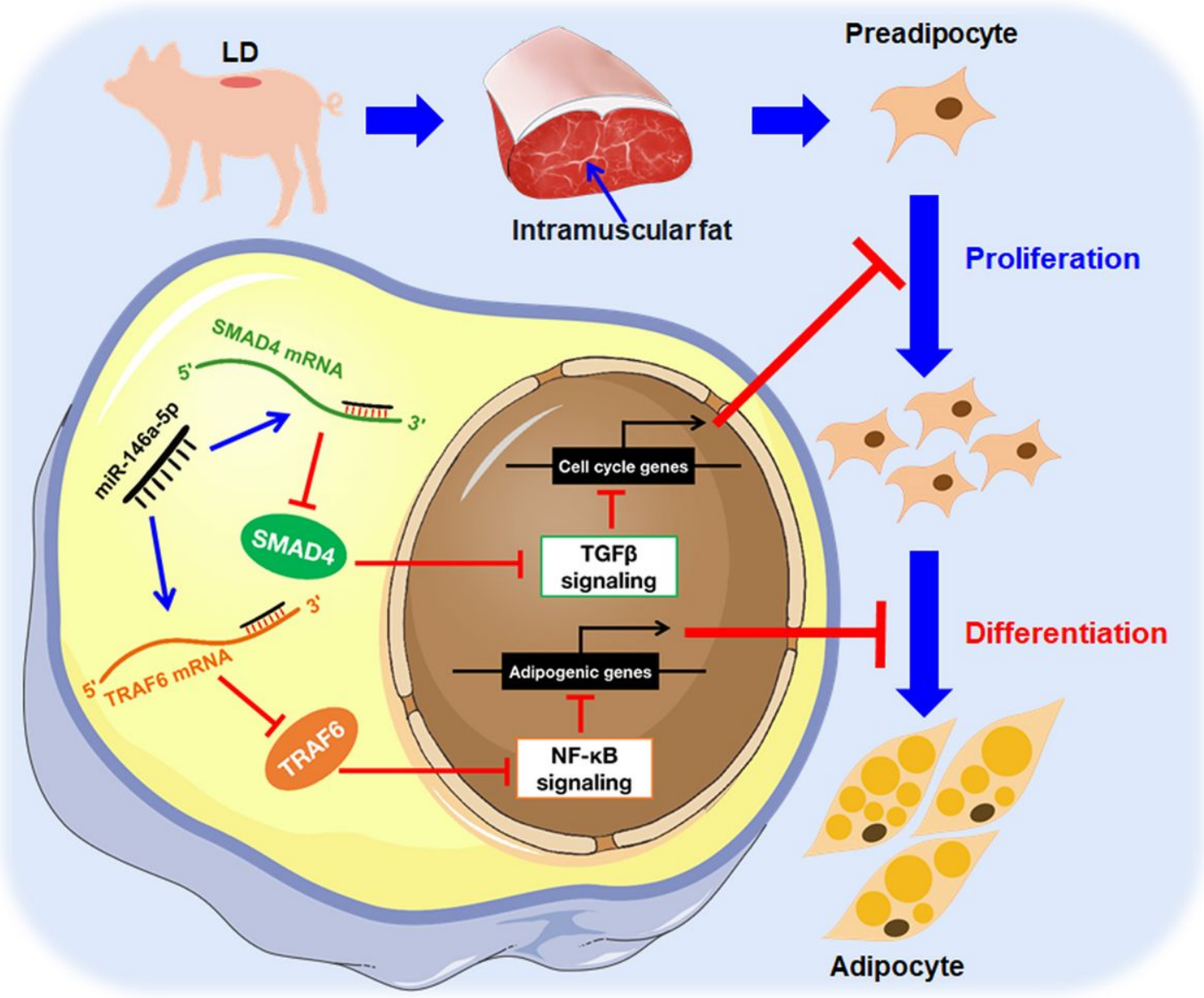

Figure 8

A model depicting the role of miR-146a-5p in regulating porcine IMF adipogenesis. The intramuscular preadipocytes are derived from the pig's longest dorsal muscle. On the one hand, miR-146a-5p targets SMAD4 mRNA, inhibits the formation of signal transduction factors, inhibits TGF-β signal transmission into the nucleus, and inhibits cell proliferation by inhibiting cell cycle related genes. On the other hand, miR-146a-5p directly targets TRAF6 mRNA to inhibit its translation and inhibits adipogenesis gene expression through the NF-kB signaling pathway, thereby inhibiting adipogenesis.